Geochemistry Geophysics Geosystems G3
AN ELECTRONIC JOURNAL OF THE EARTH SCIENCES
Published by AGU and the Geochemical Society

Article
Volume 6, Number 4
19 April 2005
Q04008, doi:10.1029/2004GC000754
ISSN: 1525-2027

Downhole magnetic measurements of ODP Hole 801C: Implications for Pacific oceanic crust and magnetic field behavior in the Middle Jurassic

Maurice Tivey
Department of Geology and Geophysics, Woods Hole Oceanographic Institution, 360 Woods Hole Road, Woods Hole, Massachusetts 02543-1542, USA (mtivey@whoi.edu)

Roger Larson
Graduate School of Oceanography, University of Rhode Island, Narragansett, Rhode Island 02882, USA

Hans Schouten
Department of Geology and Geophysics, Woods Hole Oceanographic Institution, 360 Woods Hole Road, Woods Hole, Massachusetts 02543-1542, USA

Rob Pockalny
Graduate School of Oceanography, University of Rhode Island, Narragansett, Rhode Island 02882, USA

[1] Downhole horizontal and vertical magnetic field measurements within the 474 m thick Jurassic crustal section drilled at ODP Hole 801C in the western Pacific show anomalies that are "in phase," indicating that this site formed in the southern hemisphere and moved across the paleoequator to its present location at 18.6°N. The inclination computed from the horizontal and vertical anomaly logging data varies significantly downhole and can be explained by progressive rotation of the lava sequence as it is buried during accretion. This is compatible with the observed dips in the Formation Micro Scanner (FMS) data, which show up to 42° of rotation toward the fossil spreading axis. We restore the magnetic inclination to prerotated values and obtain an estimated pretilt inclination of 39.9° ± 6.6°, corresponding to a paleolatitude of 22.7° ± 5°S. The magnetic logging data document six polarity units within the drilled volcanic extrusive crust. The upper 132 m thick logged section of lavas contains four polarity units, which apparently formed 7 Myr after the formation of the underlying basement. The lower 212 m logged section of the hole is reversely magnetized with an intervening normal polarity zone. More than one reversal downhole would indicate a rapid reversal rate given the time it takes to form the extrusive section of oceanic crust: ~45,000 years at a fast spreading rate of 66 km/Myr. Previous results from a contemporaneous section in Spain suggest rapid reversals throughout the late Bajocian–early Bathonian Stage (170–165 Ma). Nevertheless, the complicated formation history prevents quantification of the geomagnetic reversal rate for the 801C crustal section.

Components: 9430 words, 10 figures, 1 table.

Keywords: magnetism; ocean crust; Ocean Drilling Program; Hole 801C; Jurassic.

Index Terms: 1535 Geomagnetism and Paleomagnetism: Reversals: process, timescale, magnetostratigraphy; 3005 Marine Geology and Geophysics: Marine magnetics and paleomagnetics (1550); 3035 Marine Geology and Geophysics: Midocean ridge processes; 3036 Marine Geology and Geophysics: Ocean drilling.

Received 10 May 2004; **Revised** 10 January 2005; **Accepted** 24 February 2005; **Published** 19 April 2005.

Tivey, M., R. Larson, H. Schouten, and R. Pockalny (2005), Downhole magnetic measurements of ODP Hole 801C: Implications for Pacific oceanic crust and magnetic field behavior in the Middle Jurassic, *Geochem. Geophys. Geosyst.*, *6*, Q04008, doi:10.1029/2004GC000754.

1. Introduction

[2] Ocean Drilling Program (ODP) Hole 801C located in the Pigafetta basin of the western Pacific Ocean basin penetrates the oldest in situ oceanic crust drilled to date (~168 Ma) [*Koppers et al.*, 2003]. The hole is located in the Jurassic Quiet Zone (JQZ) of the Pacific plate (Figure 1) where magnetic anomalies are hard to identify in sea surface surveys partly because of attenuation due to water depth, low equatorial latitude and diurnal noise from the equatorial electrojet, but also because of the nature of Jurassic geomagnetic field behavior. The origin of the JQZ has long been the topic of vigorous debate over whether there is truly a lack of polarity reversals during this period or simply very low amplitude reversals or even very rapid reversals that would effectively cancel each other out ~6000 m away at the sea surface [*Barrett and Keen*, 1976; *Cande et al.*, 1978; *Larson and Hilde*, 1975; *McElhinny and Larson*, 2003; *Poehls et al.*, 1973; *Sager et al.*, 1998; *Steiner et al.*, 1987]. The magnetic results from Hole 801C thus represent an opportunity to investigate the origin of crustal magnetization within the JQZ. Hole 801C reaches a depth of 937 meters below seafloor (mbsf), almost 474 m deep into basement and as such provides not only important insight into Jurassic-aged crust, but also fundamental constraints on the architecture of crust created in a fast spreading environment. The hole was initially drilled during ODP Leg 129 in December 1989 penetrating 463 m of sediments and 130 m into the underlying basement [*Lancelot et al.*, 1990]. The drill-hole was reentered during ODP Leg 144 in June 1992 and was logged to 587 mbsf with a downhole magnetometer and other sensors [*Ito et al.*, 1995; *Premoli-Silva et al.*, 1993]. The hole was reentered for a third time on ODP Leg 185 during April, May 1999 and deepened to a depth of 937 m, after which a complete set of downhole logs was run [*Plank et al.*, 2000]. We report here on the analysis of downhole magnetic logs and the implications for the origin of the Jurassic Quiet Zone and the formation of ocean crust.

[3] The drilled basement section of 801C can be divided into 8 major units based on lithology, physical properties and geochemistry [*Pockalny and Larson*, 2003] (Figure 2). Sequence I (463–510 mbsf) comprises the uppermost basement and consists of late-stage alkalic basalts and doleritic sills dated by *Koppers et al.* [2003] to be 160.2 ± 0.7 Ma. Sequence II (510–530 mbsf) consists of a 20 m thick Si/Fe rich hydrothermal layer. Sequence III (530–595 mbsf) is composed of massive basaltic lava flows 1–10 m thick. Sequence IV (595–718 mbsf) consists of pillow basalts and flows with interpillow sediments and an intervening 1 m thick hydrothermal layer sequence V (625 mbsf). We separate sequence IV into IVa above this layer and sequence IVb below this layer. Sequence V appears to represent a hiatus in crustal formation with a distinct change in trend of the basalt Zr contents above and below this horizon indicating different magmatic regimes were active before and after this period [*Plank et al.*, 2000; *Pockalny and Larson*, 2003]. Dating supports this view as both sequences III and IVa give an age of 159.5 ± 2.8 Ma while sequence VI (718–840 mbsf) consists of true Jurassic basement with massive lava flows with an age date of 167.7 ± 1.4 Ma [*Koppers et al.*, 2003]. Middle Jurassic radiolarians are interbedded among these igneous units and have ages consistent with these radiometric dates [*Bartolini and Larson*, 2001; *Palfy et al.*, 2000].

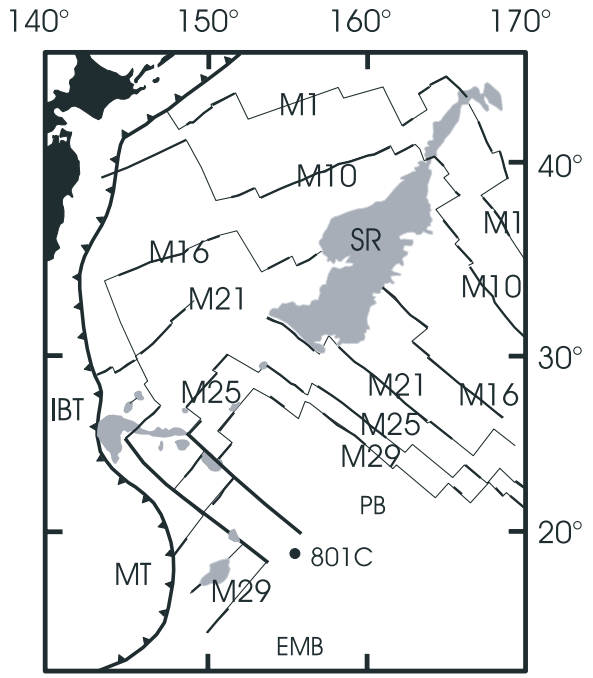

Figure 1. Chart of the Site 801C area within the Jurassic magnetic "Quiet Zone" of the Pigafetta Basin (PB) in the northwestern Pacific Basin within major magnetic isochron lines identified with their M-chron numbers. The Marianas Trench (MT) is shown by a hachured line. SR is Shatsky Rise, EMB is Eastern Mariana Basin, and IBT is Izu-Bonin Trench.

[4] Sequence VI is underlain by a 10 m thick breccia layer (840–850 mbsf) defined as sequence VII, possibly related to faulting. Finally, sequence

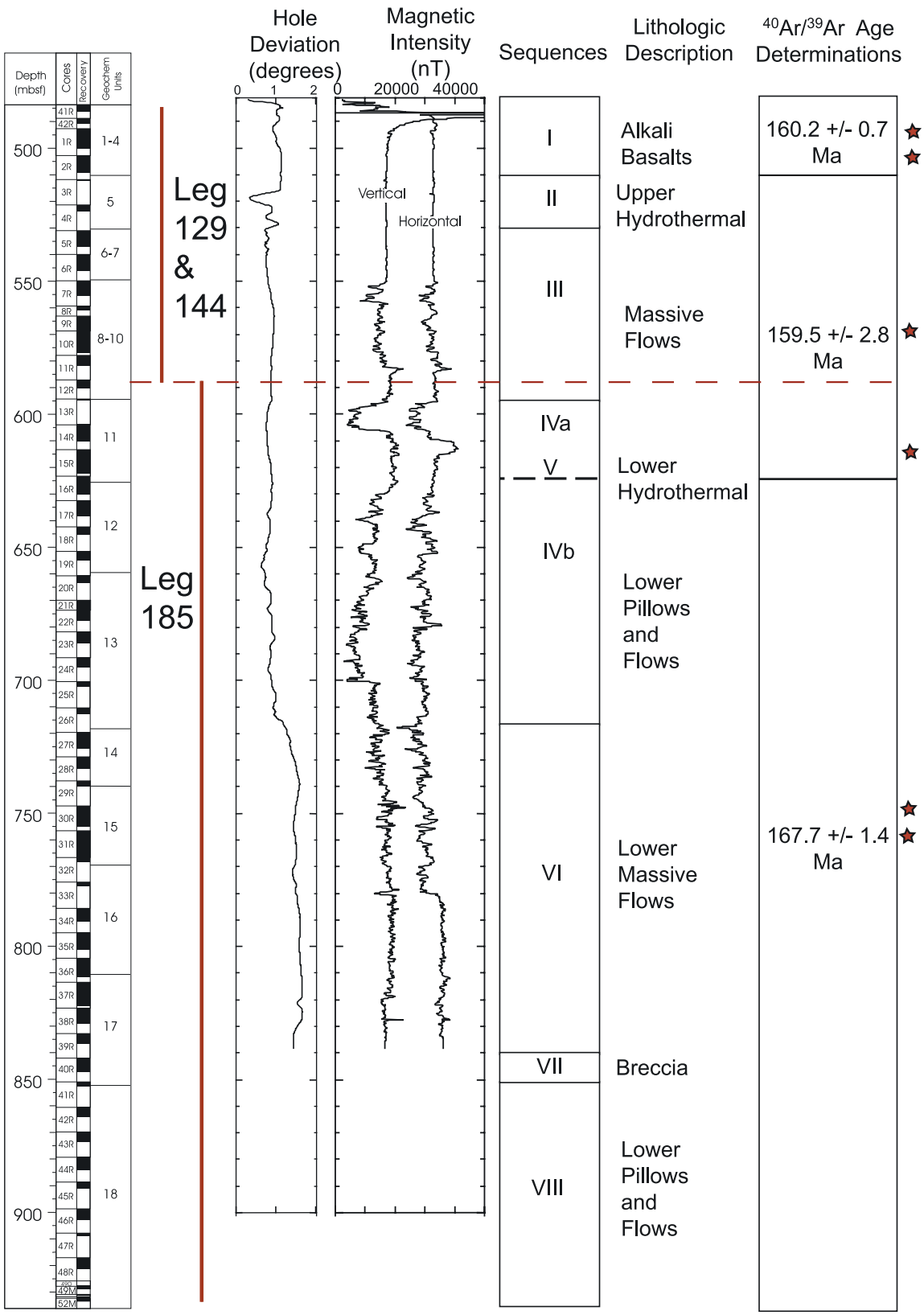

Figure 2. ODP Hole 801C core log data showing, from left to right, the proportion of core recovery (in black), the depths reached in the various drilling legs, hole inclination from vertical, magnetic logs of horizontal and vertical field components, the identified sequence units, general lithologic/petrologic unit descriptions, and the recent age determinations from *Koppers et al.* [2003]. Stars indicate the location of samples used in the age determinations.

VIII (850–936 mbsf) is the lowermost unit in the hole with thin pillows and flows (<1 m thick). The significant gap in ages of about 7.3 Myr between the alkalic and upper lavas of sequences I through IVa and the lower lavas of sequences IVb and VI suggest that additional volcanism occurred significantly off-axis following the initial emplacement of the basement lavas at the ridge axis [*Koppers et al.*, 2003].

2. Logging Measurements

[5] After coring was completed in Hole 801C on Leg 185, three-axis magnetometer logging was carried out using the General Purpose Inclination Tool (GPIT) magnetometer, which is the orientation device for the Formation MicroScanning (FMS) microresistivity tool. In nonmagnetic formations the GPIT orients the FMS data with a precision of 1° relative to magnetic north. In highly magnetized formations such as oceanic basement the magnetometer also records anomalies caused by the ambient magnetization of the adjacent borehole wall. Magnetometer logging was accomplished on two runs in Hole 801C through 344 m of volcanic basement from 493–837 mbsf (Figure 2). The upgoing log is essentially identical to the down-going log indicating the logging record is a robust and repeatable signal of the hole's magnetic properties. We use the down-going log for the calculations that follow. The tools were probably blocked at the bottom of the runs by a collapsed breccia interval at the top of sequence VII, and thus the lowermost 102 m of the hole were not logged. Concurrent hole inclination measurements show the hole to be within 2° of vertical throughout the logged interval (Figure 2).

[6] Logging of the upper part of the section from 493–587 mbsf duplicated previous measurements on ODP Leg 144 [*Ito et al.*, 1995], where a more complete instrument description is published. The downhole magnetic anomaly signatures through the duplicated interval are essentially identical in both data sets; however, we note a constant offset between the logs taken on the different legs. The horizontal component on Leg 144 averaged 32449 nT versus the Leg 185 average of 32748 nT, for a difference of 299 nT. The vertical component on Leg 144 averaged 13942 nT versus the Leg 185 average of 17018 nT for a difference of 3076 nT. We attribute these offsets to a difference in toolstring combinations. On Leg 185 the GPIT/FMS tool was configured with a sonic logging tool, while on Leg 144 it was run alone. The sonic tool used on Leg 185 apparently superimposed a constant magnetic field on the ambient anomalous field values. This field is mainly present in the vertical component, as would be expected of the field due to a long, vertically magnetized rod. To check the accuracy of the Leg 144 values, we compared the average value recorded in the "nonmagnetic" part of the formation from 500–540 mbsf (Figure 2) with IGRF (International Geomagnetic Reference Field, IAGA, 2000) values. The Leg 144 averages have total field and inclination values that are very close to the IGRF values for this location: Leg 144 total field strength = 35324 ± 177 nT versus IGRF total field strength = 35304 nT; Leg 144 inclination = 23.3° versus IGRF inclination = 22.3°, an error of 1°. The Leg 185 total field and inclination give values of 36906 nT and 27.5°, respectively, an apparent error in inclination of 5.2° compared to the IGRF value. Thus we conclude that the Leg 144 values are sufficiently accurate that they can be used to correct the Leg 185 values for the magnetic offset effect of the additional sonic tool and for the IGRF.

3. Logging Data Interpretation and Modeling

[7] Visual inspection of the vertical and horizontal magnetic field components (Figure 2) reveals a "nonmagnetic" interval at the top of the section from 493–550 mbsf where both field components record only regional field values. *Ito et al.* [1995] suggested that this nonmagnetic zone resulted from demagnetization during hydrothermal alteration that accompanied the emplacement of the alkalic basalts and the upper hydrothermal unit. The remainder of the logged interval underlying the nonmagnetic zone is a section containing a large number of short-wavelength anomalies (<10 m) superimposed on about six, long-wavelength anomalies (10–100 m) (Figure 2). These anomalies are generally present in both field components. We suspect that the short-wavelength anomalies reflect local geological variations and that the long-wavelength anomalies represent magnetic polarity units.

[8] The polarity (normal or reverse) and hemisphere of origin (north or south) of the remanent magnetization can be uniquely determined by inspecting the signs of the horizontal and vertical magnetic anomaly components (see Figure 3) [*Ito et al.*, 1995]. For a site now located in the northern hemisphere, in-phase (same signed) horizontal and vertical components indicate a southern hemisphere of formation. In addition, in-phase positive

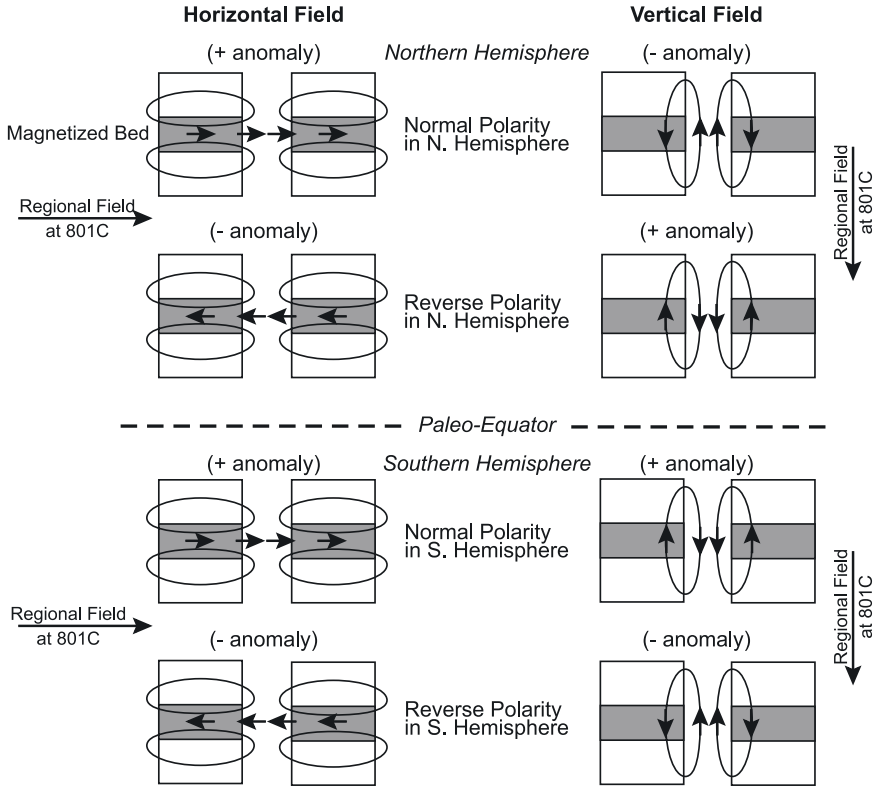

Figure 3. Cartoon showing the four different combinations of horizontal and vertical field anomalies related to the four different combinations of polarity and hemisphere of origin. The Hole 801C data show "in-phase" horizontal and vertical components indicative of a southern hemisphere of origin, i.e., both positive anomalies for normal polarity in the southern hemisphere and both negative anomalies for reverse polarity in the southern hemisphere.

anomalies in both the horizontal and vertical components indicate normally magnetized rocks, and in-phase negative anomalies indicate reversely magnetized crust formed in the southern hemisphere [*Ito et al.*, 1995]. As discussed above, we subtracted the mean value of the field in the nonmagnetic part of the hole (500–540 mbsf) from the remainder of the data to obtain the magnetic anomaly for each component (see Figures 4a and 4b), which is essentially equivalent to removing the IGRF. The six, long period anomalies, with amplitudes of 500–1500 nT, generally have "in phase" vertical and horizontal field components. On the basis of the two uppermost anomalies from 550–587 mbsf, *Ito et al.* [1995] suggested that this in-phase relationship indicates a southern hemisphere of formation for the tholeiitic basalts. This suggests subsequent tectonic transport across the paleoequator to the present-day location at 18.6°N. We agree with this interpretation and suggest that it is supported by the remainder of the magnetic logging data below 587 mbsf. Thus the interval from 550 to 583 mbsf is mainly reversely magnetized and the interval below 583 mbsf is normally magnetized (Figures 4a and 4b), which agrees with the polarities assigned to the paleomagnetic samples from those intervals [*Wallick and Steiner*, 1992]. We extend the polarity estimation analysis of *Ito et al.* [1995] to the entire downhole log record. For this polarity analysis, we compared the sign of the horizontal and vertical anomaly components from the downhole logs assigning positive polarity when both anomalies are positive and reverse polarity when both are negative. We used a cutoff total field amplitude of 2000 nT (based on the noise baseline of the total field signal) below which no polarity determination was attempted. The results are shown in Figure 4c. From this analysis, we confirm the picks of *Ito et al.* [1995] above and place the lower boundary of the normal polarity unit at 595 mbsf. We find the following additional polarity units: a reverse polarity unit between 595 and 605 mbsf, a normal polarity unit between 605 and 625 mbsf and a thick reverse polarity unit between 625 and 779 mbsf. A normal polarity unit extends from 779 mbsf to the bottom of the logs at 837 mbsf (Figure 4c). According to paleomagnetic measurements on recovered core [*Plank et al.*, 2000; *Steiner and Leg 185 Shipboard Scientific Party*, 1999] this normal polarity unit

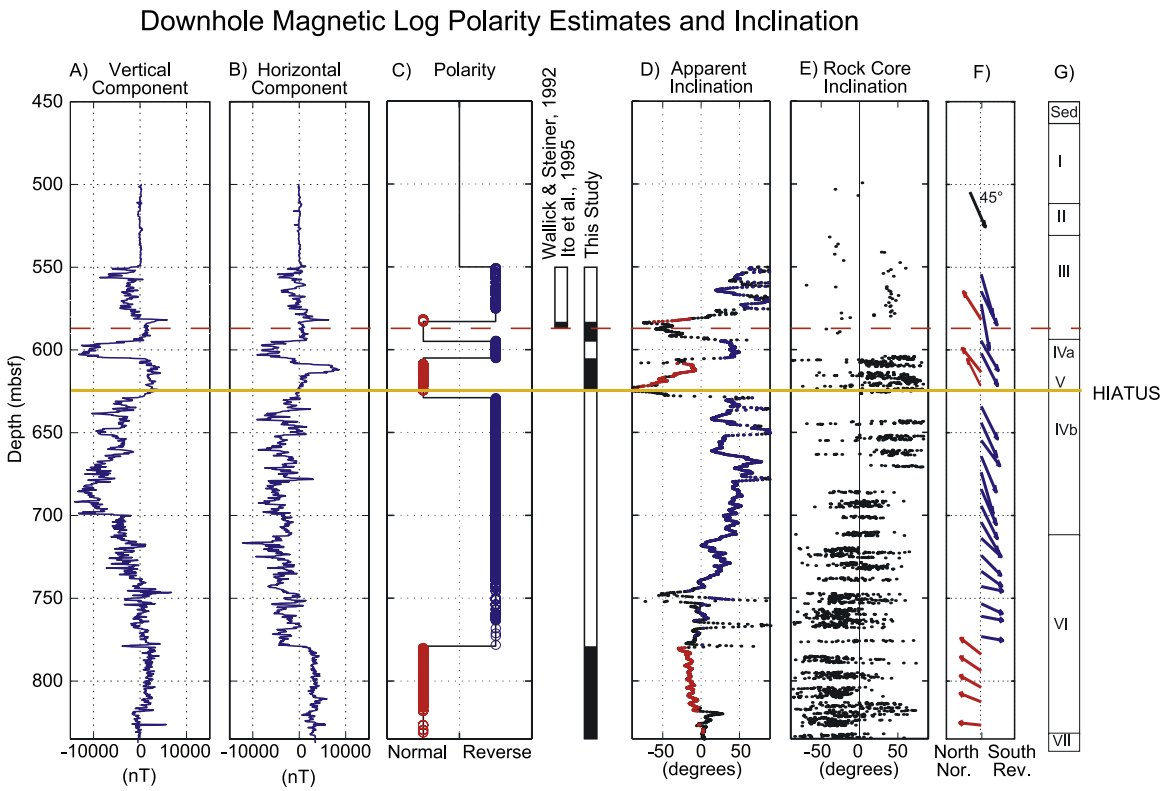

Figure 4. Downhole magnetic anomaly field for the (a) vertical and (b) horizontal magnetic field components, (c) polarity estimates based on the sign of the ratio of the horizontal to vertical components with a total field vector magnitude threshold of 2000 nT (red circles indicate normal polarity, blue circles indicate reverse polarity), and the polarity unit summary from previous work and this study, (d) calculated apparent inclination (black dots), where red dots indicate normal polarity and blue dots are reverse polarity estimates, (e) shipboard rock core NRM measurements of continuous core from Leg 185 (http://www.oceandrilling.org) and discrete sample measurements for Leg 129 [*Wallick and Steiner*, 1992], (f) diagrammatic version of computed inclination with red arrows (left-pointing) representing normal polarity and blue arrows (right-pointing) representing reverse polarity, and (g) lithologic sequence identification for reference. The red dashed line indicates the depth limit of the previous work of *Ito et al.* [1995]. The yellow solid line indicates the presumed hiatus that correlates with sequence V hydrothermal unit at 625 mbsf and the change in basement age.

extends to 875 mbsf where another reverse polarity unit begins. Thus, for the 287 m of logged basement (550–837 mbsf), we find 6 polarity units with an additional polarity unit below the logged interval. Interestingly, the polarity boundary inferred at 625 mbsf is consistent with the presumed hiatus in crustal accretion based on the age dating of *Koppers et al.* [2003]. In the deeper crustal section (i.e., below unit V) we have potentially two reversals, while in the shallow "off-axis" crustal section (above unit V) we find three reversals or four if we count the hiatus at 625 mbsf (Figure 4c). Shipboard and subsequent results from basalt samples [*Steiner and Leg 185 Shipboard Scientific Party*, 1999; *Plank et al.*, 2000; *Steiner*, 2001] indicate about the same number of reversals as in the logged portion of the 801C basalt section. The polarities determined from the logs indicate the in situ magnetization, which includes any induced component variations plus secondary magnetization effects such as viscous overprint of the present-day field and possible drilling induced remanence [*Nogi et al.*, 1995]. A magnetically soft or weakly magnetized zone could pick up a secondary drilling induced remanence. If any drilling remanence existed it would appear as a downhole component, which for the geometry here would be a reverse polarity overprint. The same is true for an induced component. There are no obvious indications of significant induced or drilling remanence problems given the close agreement with the IGRF values for the field components.

[9] Following the approach of *Hamano and Kinoshita* [1990], we can calculate the apparent inclination from the downhole log component data. A perfectly cylindrical hole radius R_1, surrounded by a larger radius R_2, horizontal cylindrical disc of

homogenously magnetized crust bounded on the top and bottom of the disc at depths Z_1 and Z_2, respectively, will have the following expression for the vertical F_Z and horizontal F_H magnetic fields in the hole at $Z = Z_0$:

$$F_H = \pi m \cos I \frac{z_0 - z}{\sqrt{(z_0 - z)^2 + R^2}} \left| \begin{matrix} z_2 & R_2 \\ z_1 & R_1 \end{matrix} \right|,$$

and

$$F_Z = -2\pi m \sin I \frac{z_0 - z}{\sqrt{(z_0 - z)^2 + R^2}} \left| \begin{matrix} z_2 & R_2 \\ z_1 & R_1 \end{matrix} \right|,$$

where z is depth, m is magnetization and I is magnetization inclination. Given that we have the IGRF-corrected, vertical and horizontal magnetic anomaly field components from Hole 801C, we can combine the above equations to solve for the apparent inclination, which is the inclination caused by a single homogenous cylindrically magnetized body for various depths in the hole. Following the approach of *Ito et al.* [1995], we define the apparent inclination I as

$$I = \arctan\left(\frac{-F_Z}{2F_H}\right),$$

where F_Z and F_H are the vertical and horizontal anomalous magnetic field components. If we make the assumption that the downhole magnetic field is dominated by remanent magnetization rather than induced field then we can calculate the apparent inclination of the crustal magnetization. Figure 4d shows the calculated result for the apparent inclination.

[10] We find again that the polarity estimates obtained from the inspection of the in-phase components are consistent with the calculated apparent inclination (Figure 4d); above 625 mbsf there are multiple reversals with a mean inclination of approx. ±40°. Our mean inclination differs from *Ito et al.* [1995], who used a slope technique to estimate an inclination of 23° for the 550–595 mbsf section. We believe this estimate is incorrect due to the inherently biased distribution of inclination data. We used the *McFadden and Reid* [1982] method to obtain a less-biased estimate of inclination data using a maximum likelihood estimate approach. Our inclination of ~40° agrees much better with the measured rock core values of 40° [*Steiner*, 2001]. Below 625 mbsf there is a monotonically decreasing inclination from ~40° to 0° with a polarity reversal at 779 mbsf. The calculated apparent inclination values (Figure 4d) are generally similar to the Leg 185 shipboard rock core natural remanent magnetization (NRM) measurements of continuous core (Figure 4e) available from the online ODP core repository database (http://www.oceandrilling.org). The main discrepancy at 610–625 mbsf is resolved after demagnetization of the rock core, which shows this zone to be weakly magnetized such that the NRM may have been overprinted in a direction consistent with a drilling remanence.

[11] These calculated inclination values represent the in situ values of the inclination, which includes the effects of postformation tilting or block rotation and tilting due to the lava burial process during crustal formation [*Schouten*, 2002; *Schouten and Denham*, 2000]. We note here that tilting and rotation of the lava sequence can make in situ inclination values change sign, i.e., an apparent change in polarity when in fact polarity has not changed at all. It is also important to recognize that as inclination becomes close to zero, it is difficult to assess the correct polarity from rock sample measurements alone, making the component data from downhole logging all the more important in defining polarity. Postemplacement tilt or block rotation is typically a rotation about an axis parallel to and away from the spreading center (i.e., a backtilt) and for Hole 801C would result in a steepening of the inclination vector regardless of polarity in the southern hemisphere. In contrast, the rotation or tilt associated with lava burial is about an axis parallel to but toward the spreading center [*Schouten*, 2002], shallowing the inclination vector regardless of polarity in the southern hemisphere. Additional data are required to correct for these effects especially in the absence of a known paleoinclination or latitude of formation. Fortunately, we have independent evidence for the structural dip of the lithologic units by utilizing the FMS data collected concurrently with the magnetic logging [*Pockalny and Larson*, 2003]. *Pockalny and Larson* [2003] calculated dips downhole at 25 m depth intervals using ''binned'' arithmetic means. They show a relatively constant dip of 15°–20° above 620 mbsf followed by a monotonic increase in dip downhole from about 20° to 40° at 800 mbsf [see *Pockalny and Larson*, 2003, Figure 5]. The binned inclination and azimuth means were incorrectly calculated separately and should be calculated using a Fisher statistical approach. We have recalculated the binned FMS data dips and azimuths in 50 m bins every 25 m

Table 1. Binned Mean FMS Dips for Downhole 801C From *Pockalny and Larson* [2003] and Recalculated Values Using Fisher Statistics for 50 m Bins Every 25 m[a]

Bin Middepth, mbsf	Original Mean Dip, deg	Original Mean Dip Standard Deviation, deg	Recalculated Dip, deg	Recalculated Azimuth, deg	Recalculated 95% Confidence Interval, deg
500	12.0	9.5	-	-	-
525	18.1	13.2	16.5	270	13.9
550	23.3	15.2	5	33	NA
575	20.3	15.0	11	67	NA
600	18.9	10.7	20	280	10.9
625	22.9	10.3	27	305	9.6
650	27.2	10.9	33	317	13.1
675	26.9	10.2	31	237	13.3
700	26.7	10.0	34	256	10.9
725	30.8	14.6	35	321	12.9
750	38.8	14.4	40	245	12.1
775	33.4	12.0	32	259	11.8
800	40.1	21.1	42	281	14.5

[a] See auxiliary material data set for original FMS data.

using the appropriate Fisher methods and show the data in Table 1. (The original FMS data from *Pockalny and Larson* [2003] are given as auxiliary material[1].) The recalculated FMS dips results in shallower dips near the top of the hole of about 5° to 16° increasing to ~40° at 800 mbsf (Figure 5a and Table 1). These revised dip data can still be interpreted as having a relative constant shallow dip (<20°) for the upper lavas units down to ~625 mbsf. Below this depth there is a nearly monotonic increase in mean dip, although strict adherence to the 95% confidence level suggests a constant dip is also possible. The dips above 625 mbsf have very scattered azimuthal directions, varying from west to northeast [*Pockalny and Larson*, 2003]. Given the significantly younger age and ambiguous, but probably off-axis formation history of this section, we have assumed no significant systematic back-tilt in the hole. Below 625 mbsf the FMS data show a monotonic increasing dip characteristic of lavas tilting due to burial (see Figure 5a) with a predominant dip azimuth toward the west and northwest [*Pockalny and Larson*, 2003], which would be toward the fossil spreading center. We can use these dip data to model the apparent inclination data obtained from the magnetic logs.

[12] The apparent inclination is in the direction of the ambient field, which is 3°E at this location and close to the geocentric dipole assumption of 0°. The original strike of the lineations is unknown so we have made the assumption that the strike is in the same general quadrant as it is today (i.e., strike northeast to southwest or approximately 25–45°E [*Tivey et al.*, 2003]). A rotation about this lineation strike would not only change the inclination, but also introduce a declination change [see *Verosub and Moores*, 1981]. As an example, using the approach of *Verosub and Moores* [1981], correction for a 10° tilt toward the spreading axis about a rotation axis striking 45° for an observed reverse polarity inclination of 40° (declination 180°) in the southern hemisphere results in a restored inclination of 45.4° and a declination of 174.5°.

[13] To illustrate the effects of rotation we constructed a forward model with an initial constant inclination of 40° along with the identified polarity reversals (Figure 5b). We subjected the model to a systematically increasing amount of burial rotation of up to 45° as indicated from the FMS data (Figure 5a). The results (Figure 5c) show that the original model inclination of 40° is progressively reduced downhole by this rotation effect to almost horizontal or near zero inclination. The rotated model inclinations are an analog to the apparent inclination data that we calculate from the downhole magnetic logs. Similarly, we can restore the rotated inclination values to prerotated values by rotating the inclination about the rotation axis. In the case of our model, we know the azimuth of the rotation axis relative to the magnetic declination and so we can perfectly restore the inclination to its original unrotated values (Figure 5d).

[14] An added complication concerns the apparent inclination calculation. The apparent inclination is calculated assuming horizontal layers, when in

[1] Auxiliary material is available at ftp://ftp.agu.org/apend/gc/2004GC000754.

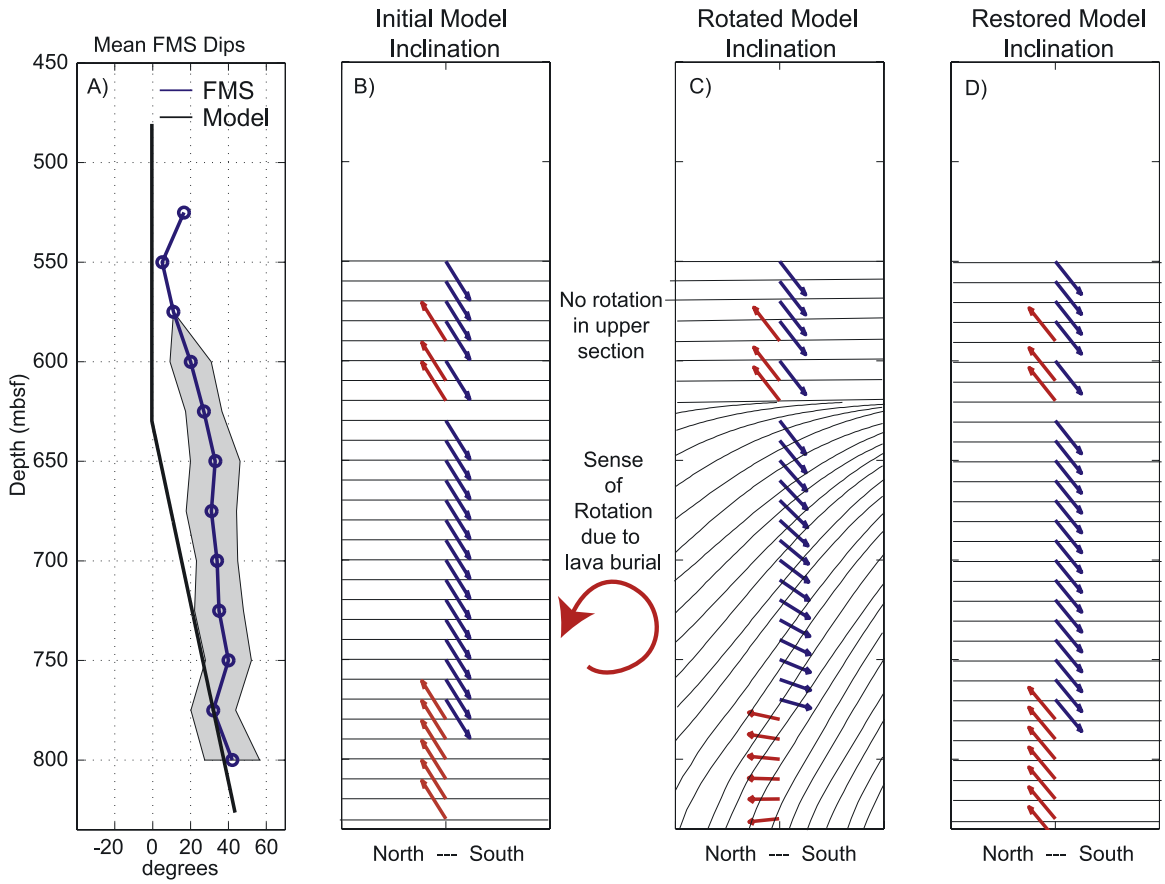

Figure 5. Forward model showing the effect of lava rotation due to burial on magnetic inclination data. (a) Computed FMS downhole dip from *Pockalny and Larson* [2003] averaged using Fisher statistical methods is shown by circles (see also Table 1) with the 95% error range indicated by the gray region. Black line shows forward model dip with zero dip above 625 m and increasing dip below this depth. (b) Initial input model inclination assumed to be 40° showing normal and reverse polarity with left-pointing arrows representing normal polarity and right-pointing arrows representing reverse polarity. Lines indicate flow units in a diagrammatic sense. (c) Rotated inclination values showing the effect of rotation due to lava burial on the magnetic inclination. Note the almost zero inclination at 779 mbsf depth. (d) Restored magnetic inclination after removal of the burial rotation effect.

fact, according to the FMS data, the layers are tilted. *Hamano and Kinoshita* [1990] give modified field equations for a tilted layer, which predict a change in shape of the magnetic field components at the boundaries. For example, a horizontal layer magnetized only in a horizontal direction will have zero vertical component. If this layer is tilted, a vertical component will be generated which will introduce an error into the inclination estimate. To determine the magnitude of this inclination error we carried out forward modeling using an ensemble of tilted layers. In this model, a series of layers progressively tilted with depth with a concomitant change in inclination, but constant magnetization shows that the error in the inclination relative to a horizontal layer estimate increases with increasing dip (Figure 6). The inclination error is also dependent on the estimated size of the contributing body to the field, R (See Figure 6). If the body is assumed to extend to infinity then the effect is substantial (70° inclination error at 50° tilt), if the body is more local then the effect is much less (<10° at 50° tilt; see Figure 6). To estimate the size of the effective magnetized zone sensed by the downhole logging we inspected the character of the observed downhole magnetic field data. The fall-off rate of a typical observed anomaly is shown in Figure 7. We find that an R value of 2 m fits the fall-off rate of the observed data better than the larger and consequently longer wavelength values of R (Figure 7). This is compatible with the analysis of *Gallet and Courtillot* [1989], who find an effective magnetic zone of about 6 times the borehole radius or ~1 m. Using a R value of 2 (about 10 times the borehole radius) implies that the error in estimating inclination due to tilt will be

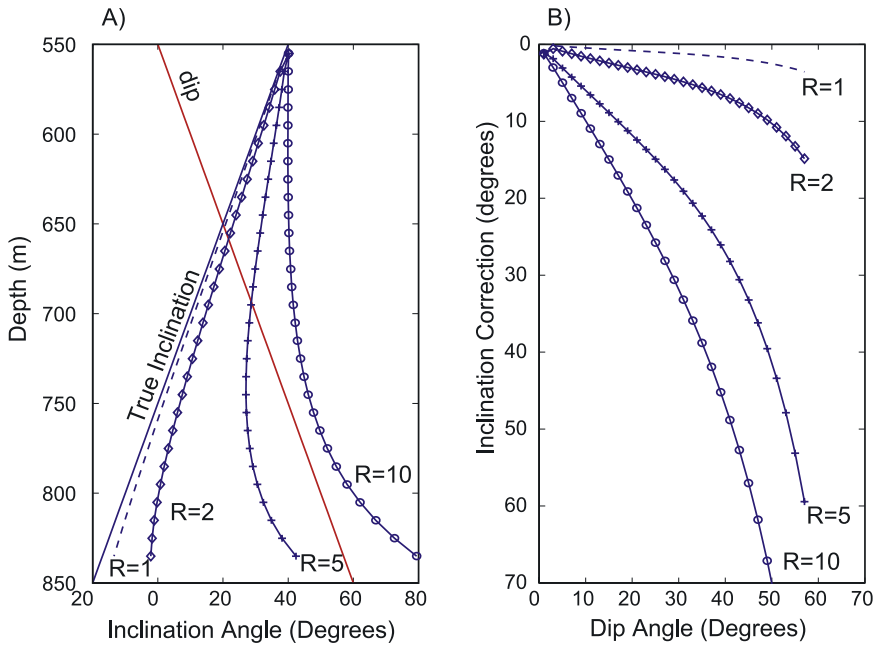

Figure 6. (a) Forward model of an ensemble of thin magnetized layers with increasing dip (solid red line) with depth. The model magnetic inclination (solid blue line) also changes as a function of the layer dip. The calculated apparent inclination shows an increasing error with depth that also changes depending on the lateral extent of the magnetized body, which varies from a radius of 1 m (dashed line), 2 m (diamonds), 5 m (crosses), and 10 m (circles). (b) Plot showing the magnitude of inclination error as a function of dip for various R values; symbol identification as before.

in the range of 0° to 10° over a tilt angle range of 0° to 50°. We can now apply this correction to the apparent inclination curve using the FMS dip data.

[15] We have now applied the dip correction and rotation modeling approach to the Hole 801C data and the calculated apparent inclination values. First, we took the absolute value of the apparent inclination data and binned the values into ~10 m bins to obtain mean values for each bin using the *McFadden and Reid* [1982] method (Figure 8b). We then applied the inclination correction for the tilt of the layers based on the FMS dip data as outlined above. We find that the corrected apparent inclination still shows a strong monotonic trend in the inclination between 650 and 800 mbsf. Again, this trend is similar to the measured rock core inclination data, which also show a monotonic decrease in inclination with depth below 650 mbsf [*Steiner and Leg 185 Shipboard Scientific Party*, 1999; *Plank et al.*, 2000]. We argue that this trend is in part due to the rotation of the magnetic vector in the lava units due to burial. It is also possible that this trend could be related to geomagnetic secular variation. For this trend to be caused solely by secular variation seems unlikely as it would mean an almost continuous eruption sequence over a short period of time in order to capture such behavior. The more likely effect of secular variation would be a general dispersion of the inclination about a mean. Given that we have independent evidence of lava tilting from the FMS data (Figure 8c), we believe that the change in inclination downhole is more reasonably interpreted as being related to rotation due to lava burial rather than systematic secular variation.

[16] We use the calculated dip from the FMS data to rotate and restore the inclination to its estimated original value. To unrotate the inclination data using the FMS dip data, we assume the rotation axis is parallel to the strike of the FMS dip, which show a west northwest directional trend (30°) relative to the magnetic field declination. We do not know the original difference in azimuth between the paleofield direction (paleodeclination) and the rotation axis and so we have assumed it was similar to today but with an uncertainty of plus or minus 45°. The rotation corrected inclination is shown in Figure 8d. The mean value of the "restored" inclination record is 39.9° ± 6.6° using the *McFadden and Reid* [1982] algorithm. This inclination infers a latitude of formation 22.7° ± 5°S.

[17] We also carried out forward modeling using the polarity and apparent inclination data to verify that we can reproduce the observed downhole magnetic field components and to qualitatively

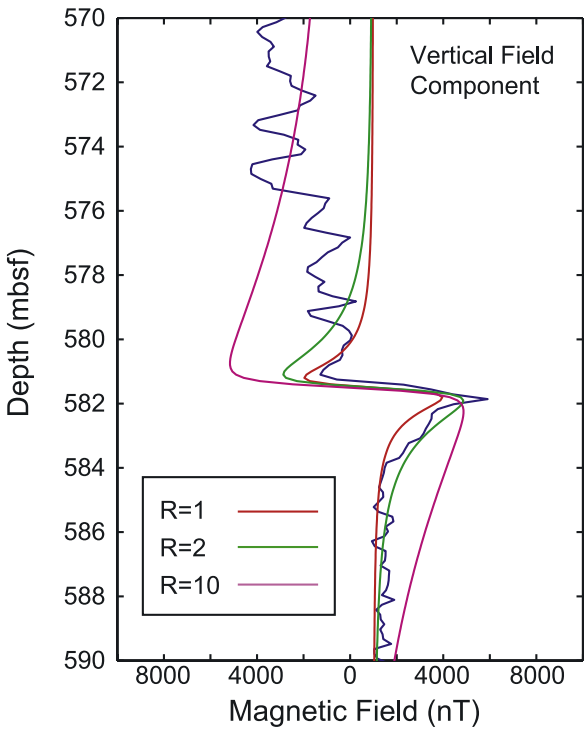

Figure 7. A fragment of the vertical magnetic field component (blue line) taken from the upper part of the 801C downhole log showing an anomaly at a polarity interface compared to forward models with varying lateral extent of the magnetized body. The best fit to the shape of the interface anomaly at 581 mbsf is approx. R = 2.

estimate the magnitude of the magnetization. We used an analytic approach to model the effects of a borehole field due to a sequence of thin horizontal layers of magnetized material [*Daly and Tabbagh*, 1988]. We ran two models each with a constant magnetization: one was at 5 A/m compatible with the NRM values reported by *Wallick and Steiner* [1992] and the other was at 10 A/m simulating stronger zones of magnetization (Figure 9). We used a smoothed version of the apparent inclination data with the same geometry for the strike of the rotation axis and declination as described earlier. On the basis of the previous arguments concerning the effect of tilted lavas we have used the raw calculated apparent inclination, which incorporates the effect of tilted lava interfaces. The modeled magnetic field is calculated assuming declination was either 0° or 180° to define the polarity information. The resultant modeled horizontal and vertical magnetic fields for the 5 A/m model correlate very well with the observed downhole magnetic field anomalies (Figure 9). Clearly, for the 5 A/m model there are some discrepancies in amplitude between the computed and observed fields, most notably near 600 and ~680 mbsf (Figure 9), which are more closely approximated by the 10 A/m model suggesting that increased magnetization at these depths could account for the stronger anomalies.

[18] Another observation is that at ~779 mbsf there is a distinct offset in the observed horizontal field anomaly (Figure 9), which goes from negative to positive downhole indicating a polarity change, while the vertical field remains relatively constant at a slightly positive value indicating no change in inclination. This is an unusual situation because for this to be an in situ reversal then inclination should change sign as well. The horizontal component nevertheless confirms this to be a reversal. We can simply take the reversal at face value and assume that observed situation is within the variability in the inclination estimates from the log data but we note that the inclination direction is not compatible with any secondary remanence produced by an induced or drilling component. Alternatively, we can suggest a more intriguing explanation for this situation in which the normal polarity unit could have been emplaced at a later time, i.e., it is an intrusive dike or sill. The inclination values are quite similar to the normal polarity units further up the hole and thus it would not have undergone the rotation due to lava burial of the main sequence. As further evidence, the FMS rotation and the calculated downhole rotation data both show a decrease below 750 mbsf. We also note here that a tectonized fault zone is identified at 840–850 mbsf. The lithologic logs [*Plank et al.*, 2000] mention no dike material at this location although core recovery is low at 779 mbsf. Below this depth there are several chilled margins and massive basalt units with no glass mentioned [*Plank et el.*, 2000]. If this unit is an intrusive dike or sill, the normal polarity of this lower unit suggests that this unit could be related to the upper lava units of sequences III and IV and thus may be ~7 Myr younger than the surrounding lava. If this is the case, then we should not interpret this unit as an independent polarity unit.

4. Discussion

[19] Analysis of the downhole magnetic field suggests that four polarity units have been logged in the upper 132 m (493–625 mbsf) of the basement, which *Koppers et al.* [2003] date to be ~160 Myr old. Polarity transitions occur at the following depths: 583, 595, 607, and 625 mbsf. This deepest polarity transition at 625 mbsf most likely indicates

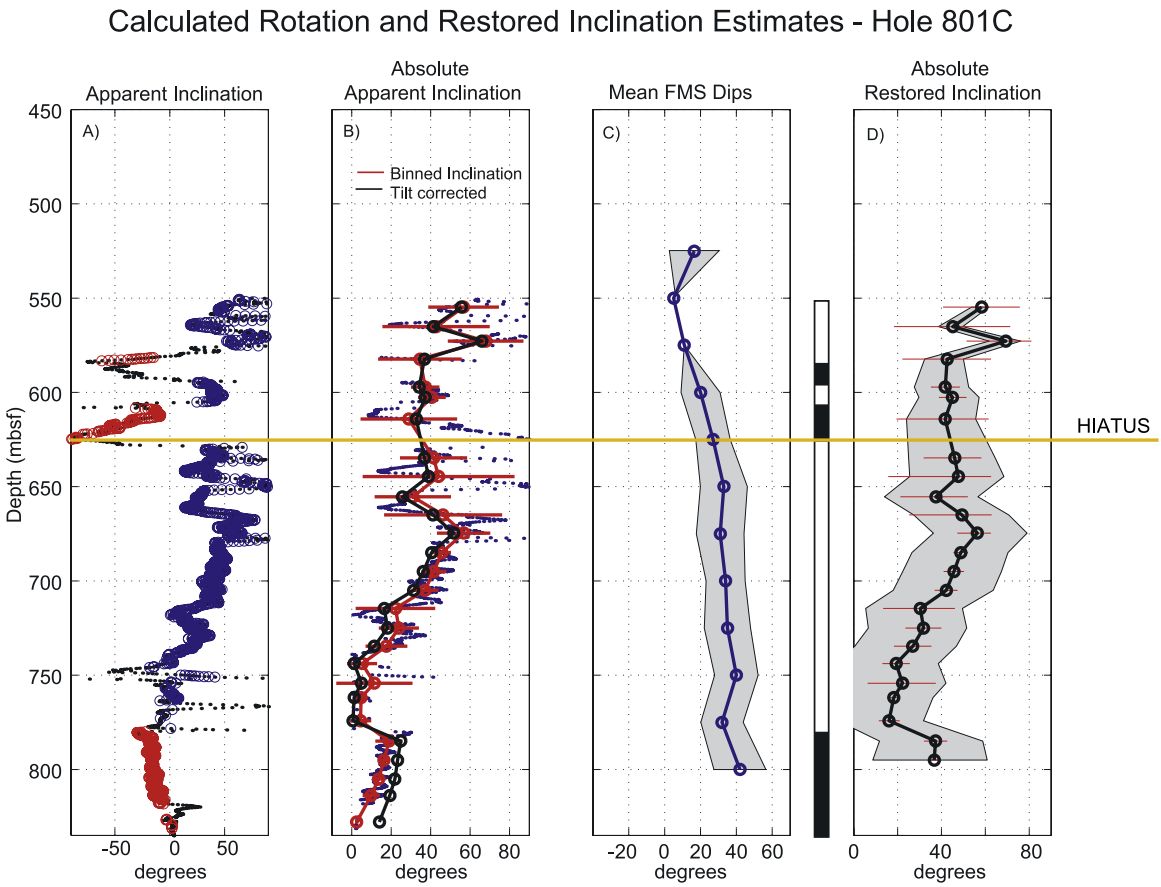

Figure 8. (a) Computed apparent inclination (black dots) based on the ratio of the horizontal and vertical field components, where red circles indicate normal polarity and blue circles are reverse polarity estimates. (b) Absolute value of apparent inclination blue dots, shown with a 10 m binned average in red circles with circular standard deviation range shown by horizontal red lines. Inclination, corrected for the tilt of the layers, is shown by the black line and circles. (c) FMS dip estimates of *Pockalny and Larson* [2003] averaged using a Fisher statistical approach (see also Table 1) shown by blue circles and adjoining line. Gray area shows 95% error confidence envelope of FMS dip estimates. (d) Inclination restored to its presumed original value (i.e., rectified) using the FMS dips shown in Figure 8c and assuming a rotation axis relative to declination of 30°. The error bars show the error in rotation from the FMS dip data, and the gray area shows the uncertainty range of ±45° in the azimuth of the rotation axis.

a hiatus of ~7.3 Myr in crustal accretion [*Koppers et al.*, 2003]. Below 625 mbsf we observe two polarity units: a reverse polarity unit from 625 to 779 mbsf and a normal polarity unit from 779 to 837 mbsf. Paleomagnetic samples indicate that a second reversal (normal to reverse) is present below the logged interval at 875 mbsf [*Steiner and Leg 185 Shipboard Scientific Party*, 1999] suggesting that there are potentially two reversals in 311 m (625–936 mbsf) of true basement. As mentioned in the previous section the true age of the normal polarity unit between 779 and 875 mbsf could be in question. This analysis is also based on the in situ magnetization and direction obtained from the logging data that could be affected by secondary magnetization when comparing directly to rock core samples (Figure 4).

[20] The multiple units of alternating polarity in both the upper lavas and the lower Jurassic basement suggest that the overall, external magnetic effect of the extrusive section will be reduced due to the canceling out of the alternating polarities down the hole. This could in part account for the reduced amplitude of the magnetic anomalies that are found in the Jurassic Quiet Zone area and in particular above the location of Hole 801C [*Sager et al.*, 1998; *Tivey et al.*, 2003]. Marine magnetic anomalies arise from the lateral variations in these polarity units and we expect the polarity units within the extrusive lavas to dip toward the fossil spreading center (~NW) due to burial associated with the crustal accretionary process [see *Tivey et al.*, 1998b]. *Poehls et al.* [1973] showed that very narrow magnetic polarity units produce model

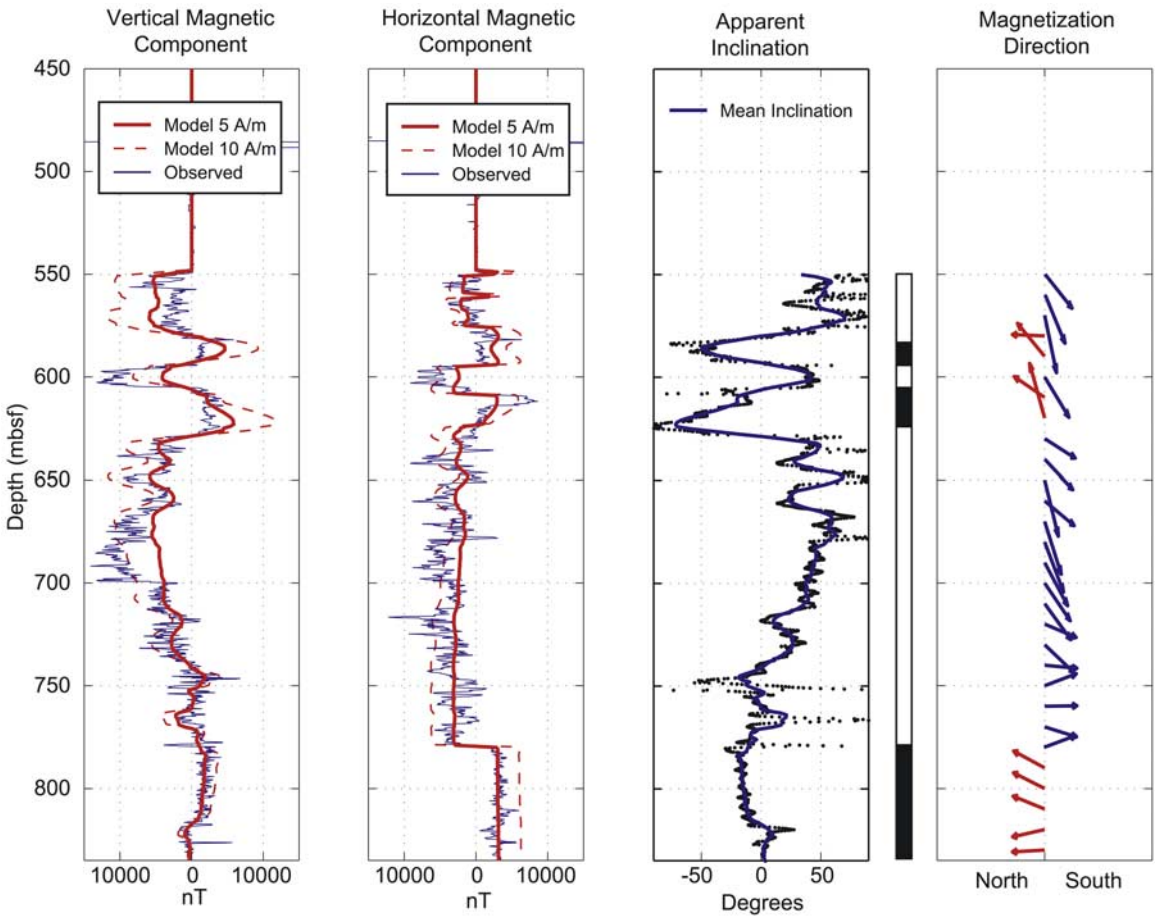

Figure 9. Forward models of the downhole magnetic anomaly field components computed using the analytic approach of *Daly and Tabbagh* [1988] assuming a constant magnetization of 5 A/m (solid) and 10 A/m (dashed). The forward modeled field is shown in red, and the measured data are shown in blue. (a) Vertical magnetic field component, (b) horizontal magnetic field component, (c) apparent inclination (black dots) and smoothed input model inclination (blue line), and (d) diagrammatic version of smoothed inclination with left-pointing arrows representing normal polarity and right-pointing arrows representing reverse polarity.

anomalies that interfere with each other and cancel out a short distance above the magnetized source, although this was for vertically sided polarity boundaries. Simply the fact of multiple polarity units occurring within a given vertical section of crust is enough to reduce the overall magnetic moment of that crust. We calculate a magnetic moment for the crustal section of Hole 801C to be 1930 Am^2, assuming an average magnetization of 5 A/m (Figure 9), but when polarity is taken into account this is reduced to an effective moment of -650 Am^2. This moment is equivalent to a 500 m thick source body with a magnetization of only $\sim$1 A/m. This weak effective magnetization provides a possible explanation for the reduction in magnetic anomaly amplitude over this region.

[21] Magnetic anomalies measured at the sea surface arise from lateral variations in magnetic polarity and intensity, so the dip of the polarity boundary [*Tivey et al.*, 1998b] and the frequency of reversals is also important to consider [*Tivey and Tucholke*, 1998]. We find that the 132 m thick upper lava units are near horizontal with little or no dip and thus these would only serve to attenuate the overall magnetic signal (Figure 10). The lower lavas have dips up to 42°, which is typical of extrusive boundaries and thus would give rise to a lateral magnetic contrasts [*Tivey and Tucholke*, 1998; *Schouten*, 2002; *Schouten and Denham*, 2000]. In terms of the reversal frequency, we can speculate on the amount of geological time represented in the logged section in Hole 801C during this portion of the Middle Jurassic. The time required to construct the extrusive oceanic crustal section at a spreading center can be estimated from the lateral distance over which the extrusive layer forms. The half-spreading rate between Hole 801C

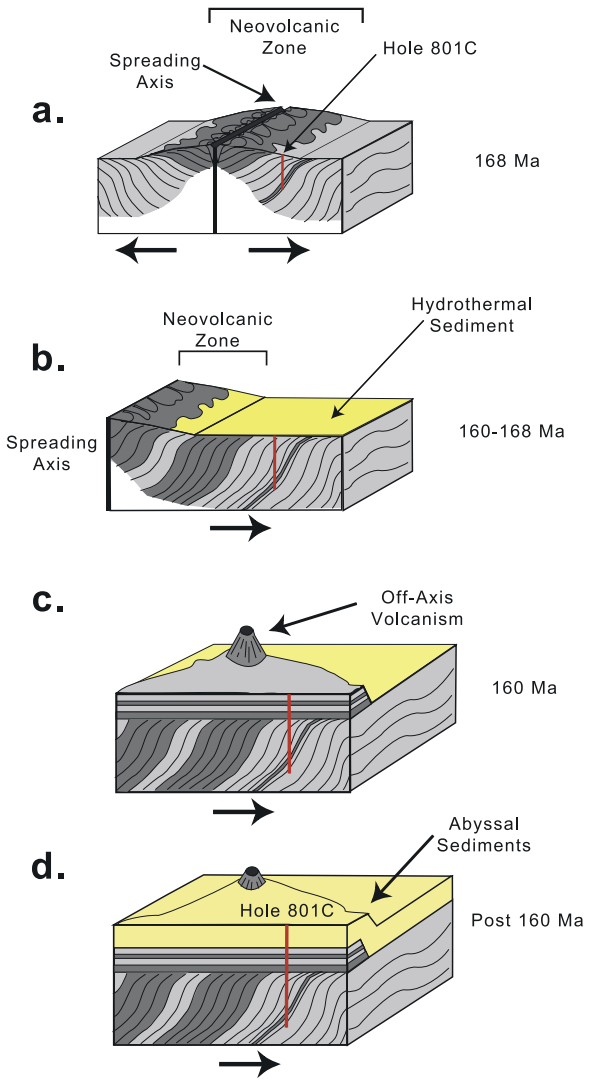

Figure 10. Cartoon showing the volcanic and magnetic history of Hole 801C; north is left, and south is right. (a) Accretion of the volcanic lava sequences VIII,VII,VI, and IVb takes place at the spreading axis within the neovolcanic zone. Lavas are progressively rotated due to lava burial. Light gray is reversely magnetized crust, while dark gray represents normal polarity (recent deeptow magnetic surveys suggest normal polarity chrons just north of the hole [*Tivey et al.*, 2003]). The youngest lavas are normal polarity, but they do not intersect the hole. (b) Formation of the Jurassic basement has ceased and a volcanic hiatus occurs in which a thin hydrothermal layer (sequence V) is deposited. (c) Off-axis volcanism (sequences III–IVa) occurs presumably from a nearby small seamount forming a ~100 m high plateau, capped by alkalic lavas (sequence I). Several polarity reversals are recorded during this period. (d) The end of volcanism and abyssal sedimentation results in burial of the volcanic basement.

(~168 Ma) and magnetic anomaly M25 (~154 Ma) gives an average half-spreading rate of 66 km/Myr [*Koppers et al.*, 2003], which is roughly equivalent to the fast spreading rate of the East Pacific Rise near 9°N (~55 km/Myr half-rate [*Carbotte and MacDonald*, 1992]). The East Pacific Rise (EPR) studies at 9°N offers insight into the crustal architecture of fast-spread crust. Seismic data show that Layer-2A, typically inferred to be extrusive crust, reaches mature thickness within 3 km of the axis [*Christeson et al.*, 1994; *Harding et al.*, 1993]. This distance, divided by the half-spreading rate (66 km/my) gives a time interval of ~45,000 years. If we consider only the lower section (below 625 mbsf) of Hole 801C to be crust accreted at the spreading center and if we estimate a typical total thickness for the extrusive layer at 801C to be 500 m, then we have penetrated ~60% (i.e., 311/500) of the section for a time interval of 27,000 years. Two polarity reversals within this time period implies a rapid reversal frequency with one reversal every ~13,500 years, which translates to a reversal rate of almost 60 rev/Myr, which is a strikingly large figure. Such a number must be taken in context, however, as this is essentially an instantaneous rate. For example, magnetic mapping on the Blanco Transform scarp of the medium spreading Juan de Fuca ridge [*Tivey et al.*, 1998a] captured the 80 kyr Jaramillo chron in a vertical cross-section and this would give an instantaneous reversal rate of 12 rev/Myr when the average is closer to 4. The high reversal rate estimated for the Jurassic crust at Hole 801C is nevertheless indicative of a high reversal rate, which is compatible with estimates based on deeptowed magnetic anomaly data of 10–12 rev/Myr for slightly younger but still Middle Jurassic crust [*Sager et al.*, 1998] and more recently collected data across the drill site location [*Tivey et al.*, 2004].

[22] An alternative view, however, is that the normal polarity unit at 779–875 mbsf is a later dike zone, which would then make any calculation of the reversal rate frequency invalid. Age dating of this unit may help resolve this issue. On the basis of initial paleomagnetic results, *Steiner and Leg 185 Shipboard Scientific Party* [1999] suggested a reversal every 100,000 to 150,000 years, which for 2 reversals implies an age of 200,000 to 300,000 years for the time to form the crust at 801C. For fast-spread crust (half-rate of 66 km/Myr) such long duration would give a crustal accretion zone of 26 to 40 km wide. This is clearly much too wide to be reasonable. However, this reversal period was subsequently revised to a value close to 10,000 years

[*Steiner*, 2001], which is consistent with our calculation. Although these very short reversal periods (large reversal frequencies) are nearly an order of magnitude shorter (larger) than others that have been measured in the past 200 Myr, very large reversal frequencies have also been inferred from continental sections of the same Middle Jurassic age [*Steiner et al.*, 1987].

[23] In the upper section of Hole 801C, the reversal rate calculations are even more speculative. There are clearly 4 polarity units within this upper 132 m of crust but as we have no model for the time involved in off-axis crustal formation, we can only guess at the period of time this crust represents. For example, if this upper crust represents 250 kyr of eruption then that implies a reversal rate of 4 rev/Myr. What is clear, however, is that this crust did not form at the spreading center, but at a distance of over 460 km from the ridge crest axis (66 km/Myr over 7 Myr). It is also possible that the hydrothermal zones in this upper section of the hole (sequences II and V, Figure 2) could also have led to remagnetization and the creation of secondary magnetization, which we now observe in situ with the logging data. The overlying alkalic basalts also infer seamount activity, although no large seamounts are found nearby with the nearest being some 100 km away, but there are small seamounts ($\sim$100 m high) and Hole 801C apparently sits on a small 100 m high plateau (Figure 10). We would not expect a coherent dipping polarity structure of the polarity units related to spreading within the crustal architecture of such a volcanic product.

[24] Certainly the section in Hole 801C is not a continuous record of Earth's magnetic field behavior because eruptions do not occur continuously, even at fast spreading centers. Thus some of these polarity intervals are probably truncated by periods when no eruptions occurred and in fact it could be argued that it is likely that all of the polarity transitions in this section are associated with hiatuses. Some polarity transitions also could have been missed completely if they occurred during a hiatus in volcanic construction. There are many cooling unit boundaries within the lithologic section that may or may not be associated with individual polarity transitions. However, there is no obvious association with any of the longer wavelength changes in the other physical or chemical logs, the most prominent occurring at 713 mbsf, where the hole inclination log (Figure 2) increases substantially above 1°. It is also possible that the number of polarity transitions has been apparently increased by later sill or dike intrusions occurring simultaneously with extrusions, causing a "doubling up" of polarity units within the section. This may be the case at 779 mbsf for example, which shows a directional change in horizontal component but not in vertical component. One explanation of this situation is a cross-cutting dike or sill related to later volcanism. The computed inclination values are similar to shallower polarity units and thus seem to support this interpretation.

[25] For all of the above reasons and uncertainties, it is impossible to calculate an exact or even an approximate reversal frequency for this section. However, the appearance of 5–6 polarity transitions in such a relatively thin oceanic crustal section certainly implies that reversals were very frequent during this portion of the Middle Jurassic.

5. Conclusions

[26] In conclusion, we find that the downhole magnetic field logging data provide a robust estimate of the reversal polarity structure within the ocean crust and potentially provides critical polarity information when inclination approaches zero. In particular, the in-phase vertical and horizontal component anomalies suggest the crust formed unambiguously in the southern hemisphere. We find multiple polarity units within the crustal section of Hole 801C. The occurrence of such multiple polarities will undoubtedly reduce the overall contribution of the cored crustal section to the overlying magnetic anomalies and thus provides a partial reason for the low amplitude of the anomalies in the Jurassic Quiet Zone at this location. Multiple polarities also infers a rapid reversal rate but the details of this are ambiguous because of the complicated formation history of the crust at 801C.

[27] Figure 10 details the magnetic history of the extrusive crust at Hole 801C. The lower 212 m of logged basement formed at or near the spreading axis within the neovolcanic zone (Figure 10a) $\sim$168 Myr ago [*Koppers et al.*, 2003]. Calculations for the formation of this extrusive crust suggest that it must form within $\sim$45,000 years. Magnetic polarity was primarily reversed but a short period of normal polarity may have been captured during this period. This normal polarity unit could also be a dike related to the younger overlying lavas. After the primary extrusive crust had formed and moved away from the spreading center a hydrothermal sediment layer accumulated (Figure 10b) followed

7 Myr later by renewed volcanism, presumably related to seamount activity. Approximately, 132 m of the logged upper basement crust contains four polarity units, which show little or no rotation (Figure 10c). There are no constraints on the duration of formation of this crust. A nonmagnetic alkalic lava unit caps this sequence followed by abyssal sedimentation (Figure 10d).

[28] The downhole log data predict significant variation in apparent inclination with depth in the hole. Although secular variation is a natural part of the geomagnetic variation we believe it is unlikely that such a serial correlation of lava eruption and field variation could be captured in this way. Instead, we suggest that the variation in inclination can be better explained by rotation of the lavas due to lava burial, i.e., toward the spreading axis. The amount of rotation due to lava burial is compatible with the observed dip of horizons measured in the FMS data. A forward model that incorporates burial and rotation of the magnetic vector with depth can explain both the downhole magnetic field data and the calculated apparent inclination downhole. We use the rotation information to restore the inclination data to its original value and to estimate an initial inclination of $\sim 39° \pm 6.6°$, which suggests a paleolatitude of formation of $\sim 22° \pm 5°$S.

Acknowledgments

[29] This research used geophysical logging data from the Ocean Drilling Program, which is sponsored by the U.S. National Science Foundation and participating countries under management of Joint Oceanographic Institutions. We thank everyone on board *JOIDES Resolution* Leg 185 for their support, and especially Maureen Steiner for scientific discussions and Logging Engineer Steve Kittredge for recording the data. We thank the reviewers Jeff Gee, Gary Acton, and Dennis Kent for their thoughtful and constructive comments, which helped improve this paper. Maurice Tivey also thanks Will Sager for his comments on an earlier draft. This research was supported by U.S. Science Support Program grants to Larson (F001114) and Pockalny (F001116) and by NSF grant OCE-0099327 to Maurice Tivey.

References

Barrett, D. L., and C. E. Keen (1976), Mesozoic magnetic lineations, the magnetic quiet zone and sea floor spreading in the northwest Atlantic, *J. Geophys. Res.*, *81*, 4875–4884.

Bartolini, A., and R. L. Larson (2001), Pacific microplate and the Pangea supercontinent in the Early to Middle Jurassic, *Geology*, *29*(8), 735–738.

Cande, S. C., R. L. Larson, and J. L. LaBrecque (1978), Magnetic lineations in the Pacific Jurassic Quiet Zone, *Earth Planet Sci. Lett.*, *41*, 434–440.

Carbotte, S., and K. MacDonald (1992), East Pacific Rise 8°–10°30′N: Evolution of ridge segments and discontinuities from SeaMARCII and three-dimensional magnetic studies, *J. Geophys. Res.*, *97*, 6959–6982.

Christeson, G. L., G. M. Purdy, and G. J. Fryer (1994), Seismic constraints on shallow crustal emplacement processes at the fast spreading East Pacific Rise, *J. Geophys. Res.*, *99*, 17,957–17,973.

Daly, L., and A. Tabbagh (1988), Towards the in situ measurement of the remanent magnetization of oceanic basalts, *Geophys. J.*, *95*, 481–489.

Gallet, Y., and V. Courtillot (1989), Modeling magnetostratigraphy in a borehole, *Geophysics*, *54*(8), 973–983.

Hamano, Y., and H. Kinoshita (1990), Magnetization of the oceanic crust inferred from magnetic logging in Hole 395A, *Proc. Ocean Drill. Program Sci. Results*, *106/109*, 223–229.

Harding, A. J., G. M. Kent, and J. A. Orcutt (1993), A multichannel seismic investigation of upper crustal structure at 9°N on the East Pacific Rise: Implications for crustal accretion, *J. Geophys. Res.*, *98*, 13,925–13,944.

Ito, H., Y. Nogi, and R. L. Larson (1995), Magnetic reversal stratigraphy of Jurassic oceanic crust from Hole 801C downhole magnetometer measurements, *Proc. Ocean Drill. Program Sci. Results*, *144*, 641–647.

Koppers, A. A. P., H. Staudigel, and R. A. Duncan (2003), High-resolution $^{40}Ar/^{39}Ar$ dating of the oldest oceanic basement basalts in the western Pacific basin, *Geochem. Geophys. Geosyst.*, *4*(11), 8914, doi:10.1029/2003GC000574.

Lancelot, Y., R. L. Larson, and Shipboard Scientific Party (1990), *Proceedings of the Ocean Drilling Program, Initial Reports*, vol. 129, Ocean Drill. Program, College Station, Tex.

Larson, R. L., and T. W. C. Hilde (1975), A revised timescale of magnetic reversals for the Early Cretaceous and Late Jurassic, *J. Geophys. Res.*, *80*, 2586–2594.

McElhinny, M. W., and R. L. Larson (2003), Jurassic dipole low defined from land and sea, *Eos Trans. AGU*, *84*(37), 362–366.

McFadden, P. L., and A. B. Reid (1982), Analysis of palaeomagnetic inclination data, *Geophys. J. R. Astron. Soc.*, *69*(2), 307–319.

Nogi, Y., J. A. Tarduno, and W. W. Sager (1995), Inferences about the nature and origin of basalt sequences from the Cretaceous Mid-Pacific Mountains (Sites 865 and 866), deduced from downhole magnetometer logs, *Proc. Ocean Drill. Program Sci. Results*, *143*, 381–388.

Palfy, J., P. L. Smith, and J. K. Mortensen (2000), A U-Pb and $^{40}Ar/^{39}Ar$ time scale for the Jurassic, *Can J. Earth Sci.*, *37*, 923–944.

Plank, T., J. N. Ludden, C. Escutia, and Leg 185 Shipboard Scientific Party (2000), *Proceedings of the Ocean Drilling Program, Initial Reports*, vol. 185, Ocean Drill. Program, College Station, Tex.

Pockalny, R. A., and R. L. Larson (2003), Implications for crustal accretion at fast spreading ridges from observations in Jurassic oceanic crust in the western Pacific, *Geochem. Geophys. Geosyst.*, *4*(1), 8903, doi:10.1029/2001GC000274.

Poehls, K. A., B. P. Luyendyk, and J. R. Heirtzler (1973), Magnetic smooth zones in the world's oceans, *J. Geophys. Res.*, *78*(29), 6985–6997.

Premoli-Silva, I., et al. (1993), *Proceedings of the Ocean Drilling Program, Initial Reports*, vol. 144, Ocean Drill. Program, College Station, Tex.

Sager, W. W., C. J. Weiss, M. A. Tivey, and H. P. Johnson (1998), Geomagnetic polarity reversal model of deep-tow

profiles from the Pacific Jurassic Quiet Zone, *J. Geophys. Res.*, *103*, 5269–5286.

Schouten, H. (2002), Paleomagnetic inclinations in DSDP Hole 417D reconsidered: Secular variation or variable tilting?, *Geophys. Res. Lett.*, *29*(7), 1103, doi:10.1029/2001GL013581.

Schouten, H., and C. R. Denham (2000), Comparison of volcanic construction in the Troodos ophiolite and oceanic crust using paleomagnetic inclinations from Cyprus Crustal Study Project (CCSP) CY-1 and CY-1A and Ocean Drilling Program (ODP) 504B drill cores, *Geol. Soc. Am. Spec. Publ.*, *349*, 181–194.

Steiner, M. B. (2001), Tango in the Mid-Jurassic: 10,000-yr geomagnetic field reversals, *Eos Trans. AGU*, *82*(47), Fall Meet. Suppl., Abstract GP12A-0205.

Steiner, M. B., and Leg 185 Shipboard Scientific Party (1999), Finally! Origin(s) of the Jurassic Quiet Zone (JQZ), *Eos Trans. AGU*, *80*(46), Fall Meet. Suppl., F507.

Steiner, M. B., J. G. Ogg, and J. Sandoval (1987), Jurassic magnetostratigraphy, 3. Bathonian-Bajocian of Carcabuey, Sierra Harana and Campillo de Arenas (Subbetic Cordillera, southern Spain), *Earth Planet. Sci. Lett.*, *82*, 357–372.

Tivey, M., and B. E. Tucholke (1998), Magnetization of 0–29 Ma ocean crust on the Mid-Atlantic Ridge, 25°30′ to 27°10′N, *J. Geophys. Res.*, *103*(B8), 17,807–17,826.

Tivey, M., H. P. Johnson, C. Fleutelot, S. Hussenoeder, R. Lawrence, C. Waters, and B. Wooding (1998a), Direct measurement of magnetic reversal polarity boundaries in a cross-section of oceanic crust, *Geophys. Res. Lett.*, *25*(19), 3631–3634.

Tivey, M. A., H. P. Johnson, and B. S. Party (1998b), Direct measurement of magnetic reversal polarity boundaries in a cross-section of oceanic crust, *Geophys. Res. Lett.*, *25*, 3631–3634.

Tivey, M. A., W. W. Sager, and S.-M. Lee (2003), Deeptow magnetic survey of the Pacific Jurassic Quiet Zone: Implication for seafloor spreading anomalies, *Eos Trans. AGU*, *84*(46), Fall Meet. Suppl., Abstract GP32A-07.

Tivey, M. A., R. L. Larson, W. W. Sager, S.-M. Lee, R. Pockalny, and H. Schouten (2004), Near-bottom seafloor spreading anomalies around Hole 801C in Pacific Jurassic crust, *Eos Trans. AGU*, *85*, *Jt. Assem. Suppl.*, Abstract GP54A-01.

Verosub, K. L., and E. M. Moores (1981), Tectonic rotations in extensional regimes and their paleomagnetic consequences for oceanic basalts, *J. Geophys. Res.*, *86*, 6335–6349.

Wallick, B. P., and M. B. Steiner (1992), Paleomagnetic and rock magnetic properties of Jurassic Quiet Zone basalts, Hole 801C, *Proc. Ocean Drill. Program Sci. Results*, *129*, 455–470.